

HIGH-RESOLUTION SIMULATIONS OF A MOON-FORMING IMPACT AND POST-IMPACT EVOLUTION

KEIICHI WADA

National Astronomical Observatory of Japan, Mitaka, Tokyo 181-8588, Japan

EIICHIRO KOKUBO

National Astronomical Observatory of Japan, Mitaka, Tokyo 181-8588, Japan

AND

JUNICHIRO MAKINO

Department of Astronomy, University of Tokyo

ABSTRACT

In order to examine the “giant impact hypothesis” for the Moon formation, we run the first grid-based, high-resolution hydrodynamic simulations for an impact between proto-Earth and a proto-planet. The spatial resolution for the impact-generated disk is greatly improved from previous particle-based simulations. This allows us to explore fine structures of a circumterrestrial debris disk and its long-term evolution. We find that in order to form a debris disk from which a lunar-sized satellite can be accumulated, the impact must result in a disk of mostly liquid or solid debris, where pressure is not effective, well before the accumulation process starts. If the debris is dominated by vapor gas, strong spiral shocks are generated, and therefore the circumterrestrial disk cannot survive more than several days. This suggests that there could be an appropriate mass range for terrestrial planets to harbor a large moon as a result of giant impacts, since vaporization during an impact depends on the impact energy.

Subject headings: planets and satellites: formation – method: numerical

1. INTRODUCTION

In the current standard scenario of planet formation, the final stage of assemblage of terrestrial planets is collisions among proto-planets of about Mars mass (Kokubo & Ida 1998; Kortenkamp et al. 2000). It is widely accepted that at this final assemblage stage, the Moon is formed from the circumterrestrial debris disk generated by an off-set impact of the proto-Earth with a Mars-sized proto-planet, which is known as the “Giant Impact (GI) hypothesis” (Hartman & Davis 1975; Cameron & Ward 1976). The initial phase of the GI scenario, a giant impact and the formation of the circumterrestrial debris disk, has been studied by a series of hydrodynamic simulations (Benz, Slattery, & Cameron 1986; Cameron 2000; Canup & Asphaug 2001; Canup 2004). N-body simulations of the accumulation of the Moon from the debris disk, which is the last phase of GI scenario, revealed that a single large moon is formed just outside the Roche limit, at a distance of about three to four times the Earth’s radius, within several months (Ida et al. 1997; Kokubo, Makino, & Ida 2000). It is believed that this GI scenario explains a number of mysteries concerning the origin of the Moon (Cameron 2000): Why is the Moon so large compared to satellites of other planets? Why is the Moon deficient in iron and volatiles compared to the Earth? Why does the Earth-Moon system have large angular momentum?

Almost all hydrodynamic simulations of GI in past decades used the Smoothed Particle Hydrodynamic (SPH) method, which is a particle-based Lagrangian scheme (Lucy 1977; Gingold & Monaghan 1977). In the SPH method, the numerical accuracy, in other words, the resolution, is determined by the number of SPH particles. The latest simulations (Canup & Asphaug 2001; Canup 2004) used $10^4 - 10^5$

SPH particles, which is an improvement of 1-2 orders of magnitude compared to simulations in the previous two decades (Benz, Slattery, & Cameron 1986; Cameron 2000). It is apparent, however, that the SPH method is not the best scheme to simulate an impact between two proto-planets. Firstly, SPH is not suitable to deal with the strong shocks and shear motion produced by the off-set impact. Moreover, since it is basically the Lagrangian scheme, the current SPH does not have resolutions fine enough for diffuse regions. This is critical problem particularly for GI, because the debris disk consists of only a few % of the total mass. As a result, even for a simulation with 10^5 SPH particles, only a few 10^3 SPH particles are used to represent the debris disk, and thus the fine structure of the disk is not resolved accurately. In the SPH formalism, the spatial resolution is determined by the ‘kernel size’, which is variable with the local density. For a diffuse circumterrestrial disk, this kernel size can be as large as the radius of the disk itself (see Figure 1 of Canup & Asphaug 2001). This is the main reason that evolution of the debris is followed for very short period (< 1 day) after the impact (Canup & Asphaug 2001). Therefore the post-impact evolution of the debris, which is a key for the GI hypothesis, is not well understood.

Alternatively, one can use grid-based Eulerian methods to overcome the above problems. Melosh & Kipp (1989) have written the only preliminary study on the GI by the grid-based method to date. However, they neglected self-gravity of the planets and debris, and the evolution is followed only for less than 1 hour around the impact. Therefore, it cannot be compared to the recent SPH simulations.

In this paper, we present the first three-dimensional hydrodynamic simulations of the giant impact followed by formation of a debris disk, taking into account the self-gravity, using a high-accuracy Eulerian-grid scheme. Our aim is to clarify the long-term (more than 100 hours after the impact) evolution of the debris with the highest numerical accuracy used in

Electronic address: wada.keiichi@nao.ac.jp

Electronic address: kokubo@th.nao.ac.jp

Electronic address: makino@astron.s.u-tokyo.ac.jp

the previous simulations for GI. We pay attention especially to effects of pressure in the debris on formation of the large moon, rather than exploring the large parameter space for the mass ratio or orbits of the proto-planets. The previous SPH simulations with $10^4 - 10^5$ particles would be fine for studying the behavior of GI for the initial several hours, and they suggest that the fraction of mass orbiting the proto-Earth just after the impact is mainly determined by the orbital parameters. On the other hand, the long-term behavior of the debris, and therefore the final mass of the moon depends on the evolution of the debris disk. It is expected that the pressure in the low-density debris should affect the hydrodynamic nature of the disk, e.g., by generating shocks. Pressure in the debris is determined by the thermodynamics and the phase-change of the material after the impact, which is not fully understood for GI (Stevenson 1987). For example, if a substantial fraction of the material is in a hot vapor form after the impact, the thermal pressure dominates dynamics of the disk, but if liquid or solid is a major component of the debris, its behavior could be very different. Since there is no practical numerical codes to treat directly two-phase flow and phase-change, we run hydrodynamic simulations assuming two extreme equations of state, which approximately represent vapor or liquid-dominated materials.

The paper is organized as follows. In §2, we briefly describe our numerical method, equations of state, and initial conditions. We show the numerical results in §3. We give conclusions and discuss an implication on a necessary condition of formation of large satellites for the Earth-type planets in §4.

2. METHOD AND MODELS

2.1. Numerical Methods

The hydrodynamic scheme used here is a standard Eulerian method, which has been widely applied to various astrophysical problems involving strong shocks in structures with a high density contrast (Wada & Norman 2001; Wada 2001). We solve the following conservation equations for mass, momentum, and energy, and the Poisson equation numerically in three dimensions:

$$\frac{\partial \rho}{\partial t} + \nabla \cdot (\rho v) = 0, \quad (1)$$

$$\frac{\partial v}{\partial t} + (v \cdot \nabla)v + \frac{\nabla p}{\rho} + \nabla \Phi_{\text{sg}} = 0, \quad (2)$$

$$\frac{\partial(\rho E)}{\partial t} + \nabla \cdot [(\rho E + p)v] = 0, \quad (3)$$

$$\nabla^2 \Phi_{\text{sg}} = 4\pi G \rho, \quad (4)$$

where, ρ , p , v , and E are the density, pressure, velocity of the matter, and the specific total energy. The gravitational potential of the matter is denoted by Φ_{sg} .

We use AUSM (Advection Upstream Splitting Method) (Liou & Stephen 1993) to solve the hydrodynamic equations and MUSCL (Monotone Upstream-centered Schemes for Conservation Laws) to achieve third-order spatial accuracy. Gravitational potential of the fluid on grid points is calculated by solving eq. (4) using the Fast Fourier Transform with a convolution method (Hockney & Eastwood 1981). These are the standard techniques for hydrodynamics taking into account self-gravity in grid-based schemes. More detailed descriptions on the numerical scheme and test calculations to guarantee the numerical accuracy are described in Wada & Norman (2001).

We use an equally spaced Cartesian grid for the computational box; $20 \times 20 \times 5$ (model A and model B) in units of r_E , where r_E is the radius of the proto-Earth. In order to see how the results are affected by a size of computational domain, we also run models in a larger domain, i.e. $40 \times 40 \times 10$ (model A' and model B'). The total number of grid points in the computational box is $512 \times 512 \times 124 \simeq 3.3 \times 10^7$ in all the models. The circumterrestrial region (i.e. $r > r_E$) is represented by $\sim 10^7$ grid points.

2.2. Equation of State

It is still an open question that what kind of equation of state (EOS) should be used in order to simulate complicated thermal and dynamical processes during GI and post-impact evolution. Conventionally two types of empirical EOS have been used with the SPH method: the Tillotson EOS (e.g. Canup & Asphaug 2001; Tillotson 1962; Benz & Asphaug 1999) and ANEOS and its extension (e.g. Melosh 2000; Canup 2004). ANEOS approximately describes mixed phase states (e.g., vapor and melt) by treating the different phases as separate components in temperature and pressure equilibrium. Note that there are no numerical simulations for GI that can handle two-phase flow consistently, and that spatial resolution must be much smaller than the system size to describe the mixed phase states. As mentioned above, it is apparent that the spatial resolutions in previous SPH simulations are insufficient to describe mixed phase states, even if they use ANEOS (see also §3.3).

One should also note that recent SPH simulations (Canup & Asphaug 2001; Canup 2004) showed that the initial behavior (i.e. a few dynamical times) of the impact does not strongly depend on choice of EOS for a given geometry of impact (i.e., mass ratio between proto-planets and the impact parameter). This suggests that the mass and the angular momentum of the debris produced by the impact, which are the most important parameters for the accumulation process of a moon, are determined by a gravitational process, not by detailed thermal processes described by the conventional EOSs.

We run a series of numerical experiments to follow a long-term (> 20 dynamical times) evolution of the debris disk. Instead of using the conventional EOSs, such as ANEOS or Tillotson EOS, we here assume two extreme EOSs: a polytrope-type EOS (EOS-1) and the same EOS, but with a zero-pressure cut-off (EOS-2). This is because assuming a simple EOS is more suitable to clarify essential physics behind the numerical results. EOS-1 is

$$p = (\gamma - 1)\rho E + C(n/3 + 1 - \gamma)\rho^{n/3+1}, \quad (5)$$

where E is the internal energy, and C is a constant. Throughout this paper, we assume the ratio of specific heats, $\gamma = 1.01$, and the constants $C = 1$, and $n = 12$. With EOS-1, the system behaves like an ideal gas or Polytropic gas at high or low temperature limits, respectively. EOS-2 is the same as EOS-1, but we introduce cut-off density ($\rho_c = 2.7 \text{ g cm}^{-3}$) and internal energy ($E_c = 4.72 \times 10^{10} \text{ erg g}^{-1}$), below which the pressure is forced to be zero in equations (2) and (3). Note that in the present problem, density in most of the debris is below ρ_0 . These numbers are the same in the SPH simulations in which the Tillotson EOS is used (Benz & Asphaug 1999). We do not adopt the ‘negative pressure’ regime assumed in the Tillotson EOS (Benz & Asphaug 1999), because it is apparently unphysical on the scale of GI. With this negative pressure regime, condensation in diffuse gas on any scales, e.g.

the scale of the Moon, is allowed, even if self-gravity of the material does not work.

The essential behavior of EOS-2 is similar to that of the Tillotson EOS. The cut-off for pressure phenomenologically represents a transition from vapor to liquid or solid particles. On the other hand, EOS-1 represents hot gaseous debris. The thermodynamical process during GI is complicated, for example, it is still unclear what fraction of the impactor is vaporized. This can be solved by a numerical scheme which can handle a two-phase (vapor and liquid) flow with elementary physics, but there is no practical code for the GI problem at this moment. We therefore perform numerical experiments for GI using hydrodynamic simulations with these two extreme EOSs to clarify the effect of pressure on post-impact evolution.

2.3. Initial Conditions

We follow Canup & Asphaug (2001) and Canup (2004) for the orbital parameters of the impactor for which the most massive satellite is expected. The masses of the proto-Earth and the impactor are assumed to be $1.0M_{\oplus}$ and $0.2M_{\oplus}$, where M_{\oplus} is the Earth mass. The radii of the proto-Earth and proto-planet are $r_E = 1.0$ and $0.64r_E$, respectively. Note that no significant differences in the results for smaller impactors (e.g. $0.1M_{\oplus}$) were found in our simulations. The initial orbits of the impactor are assumed to be parabolic, and the angular momentum is $0.86 L_{\text{graz}}$, where L_{graz} is the angular momentum for a grazing collision (Canup & Asphaug 2001). Initially the impactor is located at $4.0r_E$ from the proto-Earth.

3. RESULTS

3.1. Disk Evolution and the Predicted Lunar Mass

Figure 1 shows a typical time evolution of the giant impact with EOS-1 (model A). This model corresponds to the ‘late’ impact model in Canup & Asphaug (2001). After the first impact ($t \simeq 1$ hour), the disrupted impactor is reaccumulated to form a clump at $t \simeq 3$ hours, which finally collides with the proto-Earth at $t \simeq 6$ hours. During the second impact, the impactor is destroyed, and a dense part of the remnant spirals onto the proto-Earth ($t \simeq 10$ hours), and a circumterrestrial debris disk is formed around $t \simeq 18$ hours. It should be noted that many strong spiral shocks are generated in this process as seen in the density map (Figure 2) and azimuthal density profile (Figure 3).

Figure 4 is the same model as model A (Figure 1), but with EOS-2 (model B). The initial behavior is similar to that of model A. The impactor is completely destroyed after the second impact as is the case in model A. However, the remnant is not diffuse, but more condensed (Fig. 4) and geometrically thin (see the edge-on views). This difference is reasonable, because with EOS-2, the internal pressure does not work in the low density gas.

Next, we predict the satellite mass accumulated from the circumterrestrial disk in our models. Equation (6) is an empirical formula for the satellite mass (M_s) as a function of the specific angular momentum of the circumterrestrial disk (j_{disk}) derived from N -body experiments of lunar accretion (Kokubo, Makino, & Ida 2000):

$$\frac{M_s}{M_{\text{disk}}} \simeq 1.9 \frac{j_{\text{disk}}}{\sqrt{GM_{\oplus} a_R}} - 1.1 - 1.9 \frac{M_{\text{esc}}}{M_{\text{disk}}}, \quad (6)$$

where M_{disk} is the disk mass, a_R is the Roche limit radius, and M_{esc} is escaped mass, which is the mass lost during the accumulation process. Using eq. (6) and time-dependent mass

and angular momentum taken from our numerical results as initial conditions for the accumulation process, we plot the time evolution of the *predicted* lunar mass in Figure 5. Here $M_{\text{esc}}/M_{\text{disk}}$ is assumed to be 0.05 (Kokubo, Makino, & Ida 2000; Canup 2004). As seen in Fig. 5, the predicted lunar mass reaches a maximum of $\simeq 1.4M_L$ for model A and $\simeq 1.2M_L$ for model B just after the second impact ($t \simeq 10$ hours). However, it should be noted that the predicted mass for the model A decreases very rapidly after the lunar mass reaches the maximum on a time-scale of 10 hours. The predicted lunar mass becomes smaller than the current lunar mass M_L after $t \simeq 15$ hours, and almost monotonically declines to $0.3M_L$ at $t \simeq 65$ hours. On the other hand, if we use EOS-2 which is relevant for a mostly liquid or solid material, the lunar mass increases again after $t \simeq 40$ hours (model B). It reaches to $\simeq 0.6M_L$, and stays nearly constant until $t \simeq 90$ hours.

In a fixed-grid Euler method, a choice of the spatial resolution and size of the computational box is a trade-off. If the computational volume is not large enough, the material that escapes from the computational domain in the initial phase of the impact cannot be followed, and this could reduce the final mass of the circumterrestrial disk. In order to check this effect, we also run model B’, in which the computational volume ($40 \times 40 \times 10r_E^3$) is eight-times larger than that in model B (i.e. the grid size is twice larger than that in model B). The behavior is qualitatively similar with the result in model B, but the maximum of the predicted mass is about 1.5 time larger ($2M_L$) than that in model B. This is because that a part of remnant ‘arc’ of the impactor is lost from the computational box in model B in the initial phase of the impact (see the snapshots at $t = 14.2$ hours in Fig. 3). As a result, the predicted lunar mass in a quasi-steady state ($t > 60$ hours) is also 50% larger than that in model B. However, model B’ also shows the lunar mass does not change after $t \simeq 50$ hours, supporting the conclusion that the long-term evolution of the debris disk is followed correctly by the numerical resolution of model B’. Since the computational volume in model B’ is large enough to cover more than 90% mass of the remnant arc formed by the impact, we expect that the predicted lunar mass cannot be much larger than $0.9M_L$, even if we use a much larger computational volume with the same spatial resolution in model B. Similarly, model A’ covers 8 times larger volume than model A, and the peak lunar mass is 1.6 times larger than the one in model A. However, it also shows rapid decrease of the lunar mass, which is in contrast with the behavior in model B and B’.

3.2. Angular Momentum Transfer by Spiral Shocks

The reason why the predicted lunar mass cannot stay nearly constant after the impact in model A is clear. As seen in Figures 2 and 3, spiral shocks are generated in the debris disk. Figure 3 shows that at least two clear shocks are present for the same radii (i.e. $\phi = 0.2\pi$ and 1.95π for $r = 2.9r_E$ and $\phi = 0.5\pi$ and 1.5π for $r = 5.0r_E$). The density jump at each shock is a factor of 4 to 16, suggesting that the effective Mach number in the model is about 2 to 4. In fact, a significant fraction of the debris is supersonic in model A. Figure 6, which is a frequency distribution of Mach number \mathcal{M} in the debris at two different epochs, clearly shows that $\mathcal{M} > 6$ (mass-weighted) or $\mathcal{M} > 3$ (volume-weighted) in majority of the debris at $t = 12.3$ hours. Even in a later stage, i.e. $t = 57.1$ hours, the disk is still supersonic $\mathcal{M} \gtrsim 2$.

Due to these shocks in the gaseous disk, the inner massive

disk inside the Roche limit effectively falls onto the proto-Earth in a few rotational periods (see discussion below). This initial fall of the disk cannot be avoided in the GI process, if majority of the debris is in a hot gas phase. Since the collision should be off-set, the generation of the spiral shocks is inevitable in a vapor gas disk with a high Mach number.

The angular momentum transfer by the spiral shocks is more effective for stronger shocks with larger pitch angles (i.e., more open-spirals). We simply estimate it as follows. For isothermal shocks, the post-shock velocity is $\sim v_0/\mathcal{M}^2$, where v_0 is pre-shock velocity of the gas, perpendicular to the shock front. Therefore the stream line is bent by passing an oblique shock (see Fig. 12 and Appendix in Wada & Koda 2004). In a rotating medium, this effect removes the angular momentum of a fluid element when it passes a standing spiral shock. The angular momentum change due to one passage of a spiral shock can be approximately estimated by

$$j/j_0 \approx \left(\frac{\sin^2 i}{\mathcal{M}^4} + \cos^2 i \right)^{1/2} \cos \left[i - \arctan \left(\frac{\sin i}{\mathcal{M}^2 \cos i} \right) \right], \quad (7)$$

where i is the pitch angle of the spiral shock, j_0 and j are the angular momentum of pre- and post-shock flow (Wada & Koda 2004). The sound velocity of SiO₂ gas with 2000 K is 0.6 km s⁻¹ for 100% vapor, and $\simeq 0.1$ km s⁻¹ if the mass ratio between vapor and liquid is 0.1 (Stevenson 1987). For strong shocks ($\mathcal{M} \gg 1$), the angular momentum change, equation (7), is $j/j_0 \sim \cos^2 i$. Therefore, the angular momentum loss is $\simeq 12\%$ per spiral shock with $i = 20^\circ$. For weak shocks (e.g., $\mathcal{M} = 2$), equation (7) suggests that the angular momentum loss per shock is about 5.6% for $i = 20^\circ$ and 1.4% for $i = 10^\circ$. As shown in Fig. 2 and Fig. 3, several spiral shocks are generated in the debris disk, then a fluid element would lose $\sim 10\%$ of its angular momentum for one rotational period. This is large enough for the debris gas to lose most of their angular momentum in 100 hours after the impact. Therefore, the presence of spiral shocks in the debris disk is crucial for evolution of the disk, and as a result for the mass of satellites.

3.3. Comparison with Previous SPH Results

Remarkably, although we use methods, resolutions, and equations of state different from previous SPH simulations, the predicted mass just after the impact is consistent with recent SPH results: 1.7–1.8 M_L for the ‘late impact’ model (Canup & Asphaug 2001; Canup 2004). This again implies that the early phase of the impact process ($t \lesssim 10$ hours) is dominated by gravity, but not by hydrodynamical and thermal processes. However, we find that behavior of the remnant and the predicted lunar mass in the late phase depend on EOS, especially whether pressure works in the disk. This was not pointed out by the previous SPH simulations. One obvious reason is that the spatial resolutions in the SPH results are not fine enough to follow long-term evolution of the debris until the effect of pressure becomes evident. In the previous SPH simulations (Canup 2004), only $\sim 10^3$ particles are used to represent the debris. Suppose 1000 SPH particles are uniformly distributed in a thin disk inside the Roche limit ($3r_E$), the average separation between particles is $\simeq 0.2r_E$. In SPH, variable kernels are often used, and the kernel size is roughly the same as the spatial resolution. Usually an SPH particle is assumed to interact with 30–50 neighbor particles. Therefore, the kernel size in the previous SPH simulations, may be $\sim r_E$ in the disk, which is about 10–20 times larger than

our grid size. Moreover, the debris has in fact an extended distribution, rather than a thin disk, and the SPH kernel size is much larger than the numbers estimated above. It is not straightforward to compare the spatial resolution between the two different schemes, but apparently that the spatial resolution in our simulation is greatly improved from the previous ones. For example, in Figure 3, the azimuthal density profile is obtained by about 1000–2000 grid points. However, in the previous SPH simulations, only 10–100 particles would be available for drawing this kind of density profile.

The other reason why the previous studies did not notice the effect of shocks is that the conventional EOSs (ANEOS and Tillotson) are close to our EOS-2, in a sense that pressure is not effective in the diffuse debris.

4. CONCLUSIONS AND DISCUSSION

We run for the first time three-dimensional grid-base hydrodynamic simulations of the giant impact between proto-Earth and a proto-planet taking into account self-gravity. We assume two types of the equation of state that phenomenologically represent hot gaseous material or liquid/solid material. Our numerical experiments suggest that in order to form a lunar-sized satellite from the circumterrestrial debris disk produced by the giant impact, the most fraction of the debris should not be in a pressure-dominated phase (e.g., hot vapor gas). Otherwise the subsequent disk evolution results in forming only a small satellite because of the fast angular momentum transfer associated with spiral shocks prior to the satellite accretion stage. The time-scale of the angular momentum transfer is an order of 10 days, therefore the accumulation to form a large satellite should be much faster than this. Yet our results may not rule out a possibility forming a satellite as large as the Moon from a pressure-dominated disk, if the disk mass is much larger than the current lunar mass. This might be the case for collisions with a massive impactor, but this causes another problem on a fraction of vapor in the debris (see discussion below).

In agreement with the previous SPH simulations (e.g., Canup & Asphaug 2001; Canup 2004), we find that the predicted lunar mass at $t \simeq 10$ hours after the collision does not strongly depend on choice of EOS and numerical methods for the same orbital parameters. This means that the early phase of GI is dominated by a gravitational process, not by thermodynamical processes. On the other hand, the late phase of GI, i.e., evolution of the debris disk, is sensitive to EOS, especially the pressure in the disk. In order to clarify this difference, the spatial resolutions of the previous SPH simulations were apparently not fine enough.

Our results give an important implication on a necessary condition for formation of large satellites for the Earth-type planets. The present results suggest that one of the important keys for GI scenario is the fraction of the vaporized debris after the giant impact. If the kinetic energy of the collision is much larger than the latent heat of the major component of the proto-planet, most of the proto-planet could be vaporized by the impact. If this is the case, the disk evolution would not lead to formation of a large moon as explained above. On the other hand, if the impact velocity is slower than a critical value, a large fraction of the material can be in a liquid or solid phase, and shocks do not dominate the angular momentum transfer in the debris disk. In this case, the post-impact evolution of the proto-planet could be similar to that in model B in our experiments, and therefore a single large moon could be formed. By assuming the impact is head-on and compar-

ing the latent heat of SiO₂ (Stevenson 1987) and the kinetic energy of the impact, we can roughly estimate the critical impact velocity as $\simeq 15 \text{ km s}^{-1}$, which is slightly larger than the surface escape velocity of the Earth. In the grazing impact between proto-Earth and a Mars-sized proto-planet, shocks propagating in the planets involve vaporization, and its velocity is probably comparable (or smaller) to this critical value, and therefore it would be natural to postulate that most of the debris mass is in a liquid phase. This argument leads to an interesting suggestion: if the impact velocity is larger than the critical velocity, in other words, the mass of the planet is larger than, say, a few Earth mass, the giant impact never results in forming a large satellite.

Finally, one should recall that a correct phase-change even for the major component, such as SiO₂, during GI followed by formation of a debris disk is still unknown (e.g. Stevenson 1987). For example, the post-impact expansion could pro-

duce more vapor in the debris material, and this may change the hydrodynamic property of the circumterrestrial disk. The final fate, namely whether the planet has satellites, and how large they are, depends on the nature of the phase-change. The thermo-dynamical process during catastrophic impact between the proto-planets is still too complicated to be explored using current numerical techniques including the SPH and grid-based methods. This ultimately requires a self-consistent numerical scheme to simulate two-phase flow taking into account the realistic thermodynamical processes.

We are grateful to Yutaka Abe for his fruitful comments. Numerical computations were carried out on Fujitsu VPP5000 at NAOJ. The authors also thank the anonymous referee for his/her valuable comments and suggestions.

REFERENCES

- Benz, W., Slattery, W. L. & Cameron, A. G. W. 1986, *Icarus*, 66, 515
 Benz, W., Asphaug, E. 1999, *Icarus*, 142, 5
 Cameron, A. G. W. & Ward, W. R. 1976., *Proc. Lunar Planet. Sci. Conf. 7th*, 120
 Cameron, A. G. W. in *Origin of the Earth and Moon*(eds Canup, R. M. & Righter, K.) 133-144 (Univ. Arizona Press, Tucson, 2000)
 Canup, R. M. & Asphaug, E. 2001, *Nature*, 412, 708
 Canup, R. M. 2004, *Icarus*, 168, 433
 Gingold, R. A., Monaghan, J. J. 1977, *MNRAS*, 181, 375
 Hartman, W. K. & Davis, D. R. 1975, *Icarus*, 24, 504
 Hockney, R. W., Eastwood, J. W. 1981, *Computer Simulation Using Particles* (New York : McGraw Hill)
 Ida, S., Canup, R. M. & Stewart G. R. 1997, *Nature*, 389, 353
 Kokubo, E & Ida, S. 1998, *Icarus*, 131, 171
 Kokubo, E., Makino, J. & Ida, S. 2000, *Icarus*, 148, 419
 Kortenkamp, S.J., Kokubo, E., & Weidenschilling, S.J. 2000, in *Origin of the Earth and Moon*, ed Canup, R. M. & Righter, K. (Univ. Arizona Press, Tucson), 85.
 Liou, M., & Stephen C. J. 1993, *J. Comp. Phys.*, 107, 23
 Lucy, L. B. 1977, *AJ*, 82, 1013
 Melosh, H. J. & Kipp, M. E. 1989, in *Lunar Planet Sci. Conf.*, XX, 685
 Melosh H. J. 2000, *31st. Lunar Planet. Sci. Conf.* , ed. C. Agee & D. Block (Houston; Lunar Science Inst.) 1903
 Stevenson, D. J. 1987, Origin of the Moon - The collision hypothesis, *Ann. Rev. Earth Planet. Sci.*, 15, 271
 Tillotson, J. H. 1962, Metallic equation of state for hypervelocity impact. Report No. GA-3216, July 18 (General Atomic, San Diego, California)
 Wada, K., & Koda, J. 2004, *MNRAS*, 349, 270
 Wada, K., Norman, C. A. 2001, *ApJ*, 547, 172
 Wada, K. 2001., *ApJ*, 559, L41

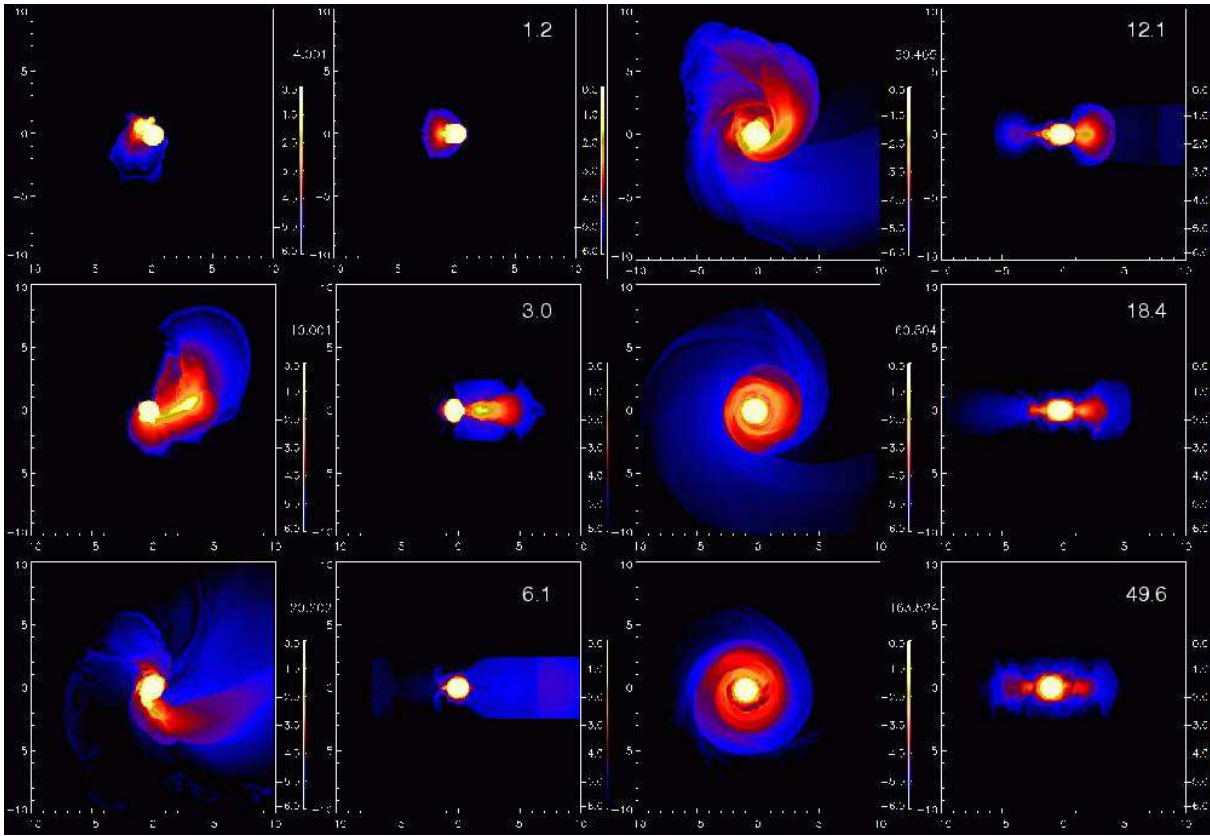


FIG. 1.— Giant impact simulation with EOS-1, which represents a state where most of the impactor mass is vaporized. The panels in the left and right rows are face-on and edge-on views of the system, respectively. The figures in the panels show the time in units of hours. The color represents log-scaled density (The unit is $\rho_0 = 12.6 \text{ g cm}^{-3}$).

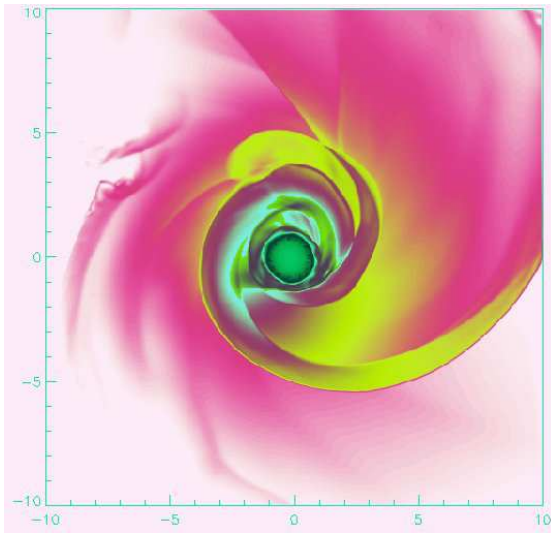


FIG. 2.— Snapshot of the density field of model A at $t = 12.3$ hours. Strong spiral shocks in the debris are resolved.

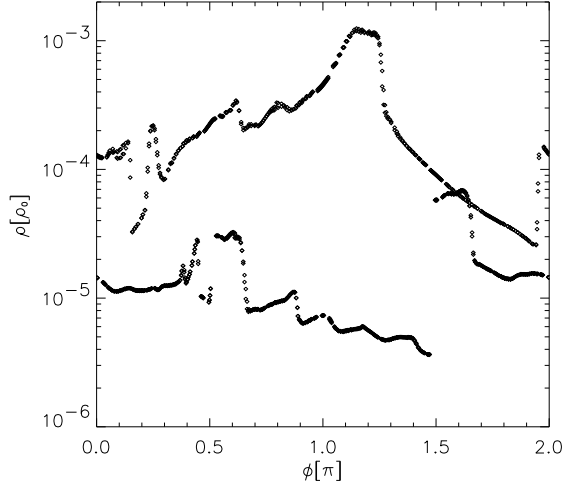


FIG. 3.— The azimuthal density profiles at $r = 2.9 r_E$ (upper dots) and $5.0 r_E$ (lower dots) on $z = 0$ plane for the same density snapshot in Fig. 2. The unit of density is $\rho_0 = 12.6 \text{ g cm}^{-3}$.

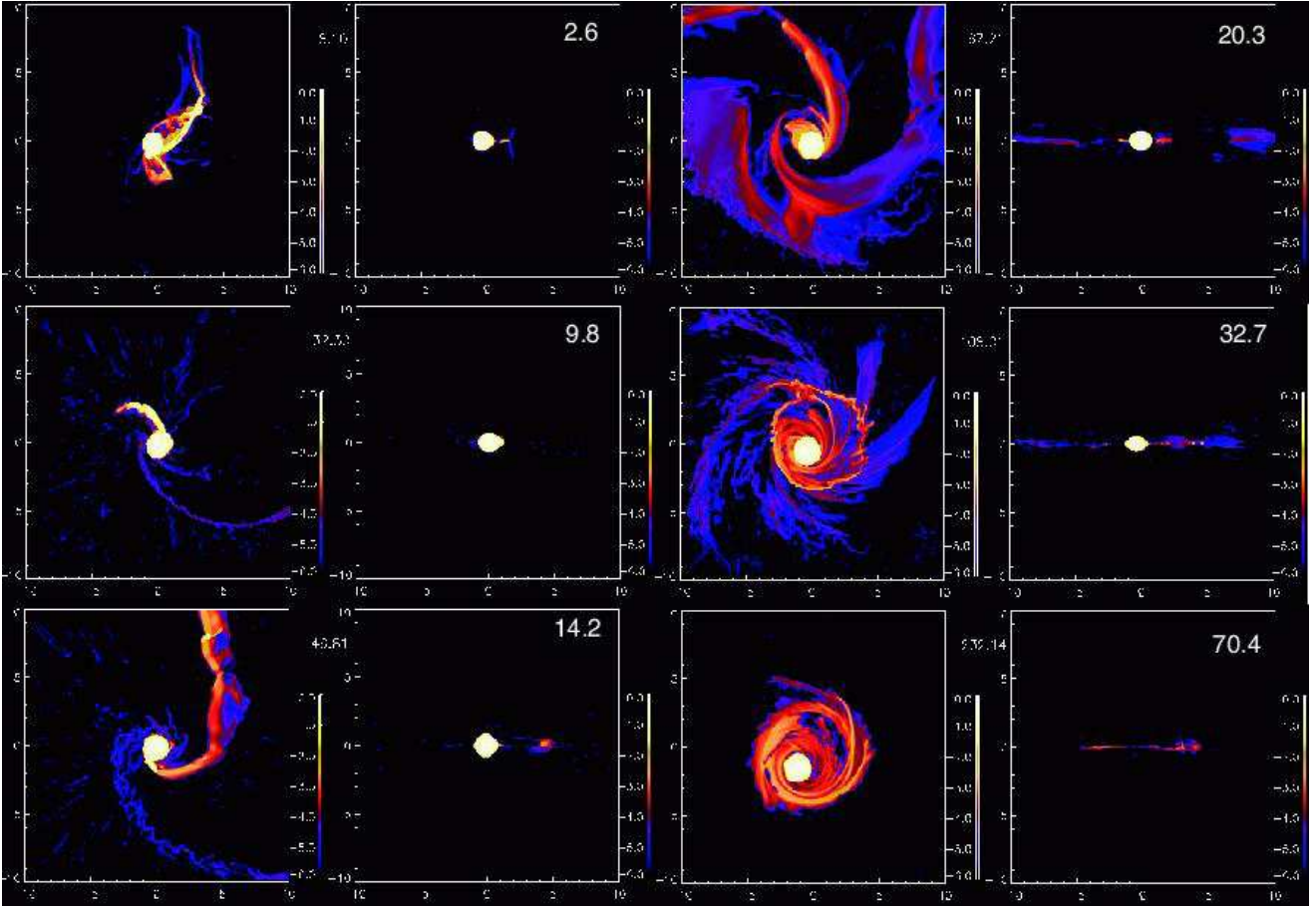


FIG. 4.— Same as in Figure 1, but for model B, in which zero-pressure EOS (EOS-2) is assumed. Following previous simulations with the Tillotson EOS (Tillotson 1962), we adopt the cut-off density ($\rho_c = 2.7 \text{ g cm}^{-3}$) and internal energy ($E_c = 4.72 \times 10^{10} \text{ erg g}^{-1}$), below which the pressure is forced to be zero in EOS-1. The EOS-2 represents a state where most of the mass is in a state of liquid, not in vapor.

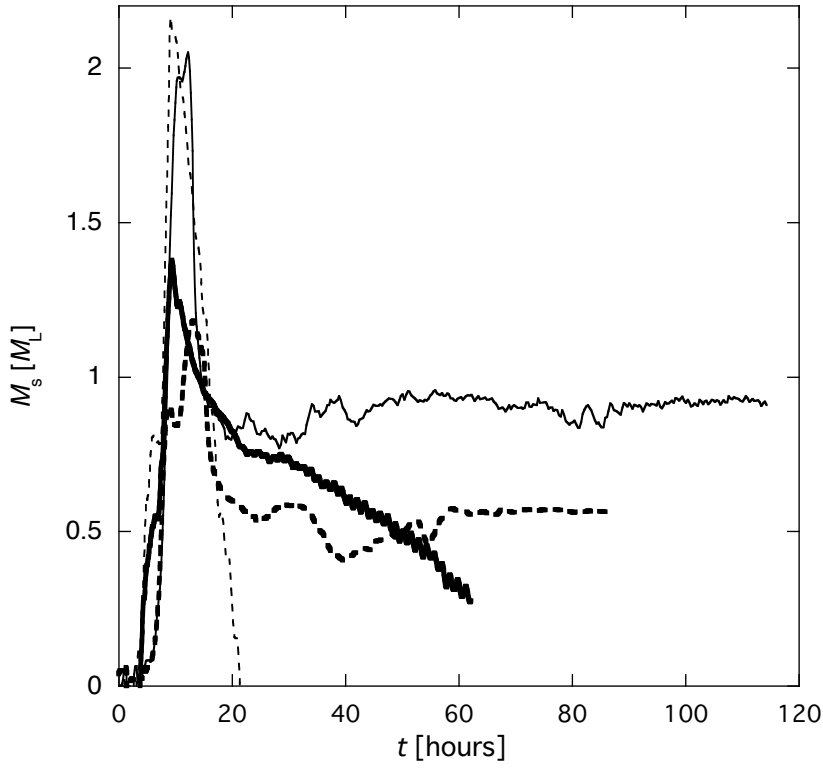


FIG. 5.— Evolution of the predicted lunar mass (M_s) in model A shown in Figure 1 (thick solid line) and model B in Figure 4 (thick dashed line). The vertical axis is normalized by the current lunar mass ($M_L = 0.0123M_\oplus$). The thin dashed and solid lines show models A' and B', in which the computational volumes are eight-times larger than those in models A and B.

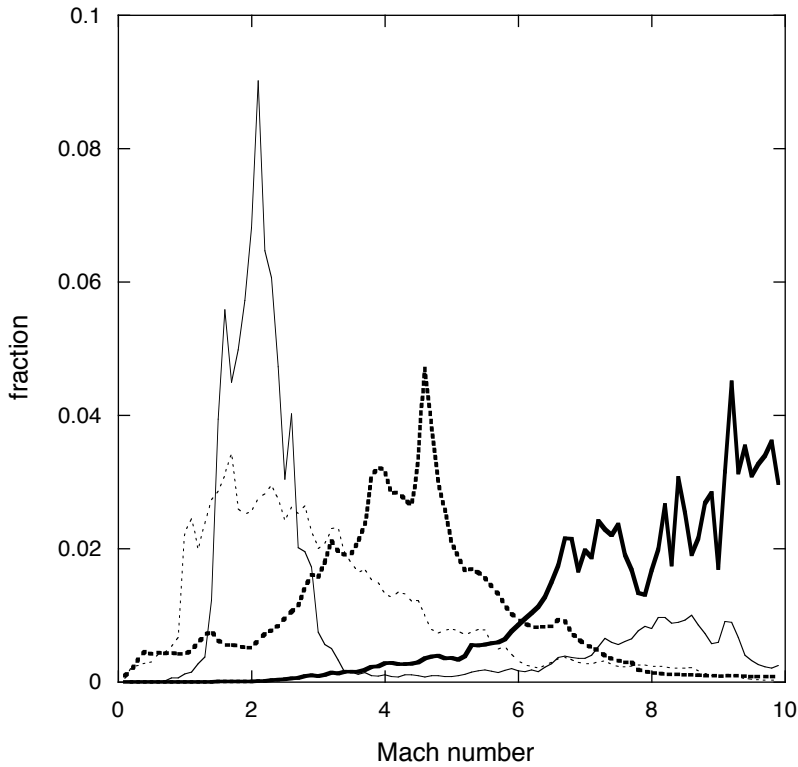


FIG. 6.— Frequency distribution of Mach number in the debris ($\rho < 0.1\rho_0$) of model A. Thick lines are at $t = 12.3$ hours. Thin lines are at $t = 57.1$ hours. Solid and dotted lines are mass-weighted and volume-weighted histograms, respectively.